

Calculating Two-Dimensional Chemically Reacting Flows

CARL SCACCIA*

Union Carbide Corporation, Tonawanda, N.Y.

AND

LAWRENCE A. KENNEDY†

State University of New York at Buffalo, Buffalo, N.Y.

In the integration of chemically reacting flows, the species, and energy equations present stability difficulties in their numerical solutions because of their coupling with the kinetic source terms. Such equations are termed stiff. Two methods for handling these equations for multidimensional flow problems are examined and applied to an H_2O_2 reaction in a two-dimensional flow.

Nomenclature

C_p = specific heat
 h_i = enthalpy of species i
 k = specific rate constant
 L = characteristic length (width of chamber)
 Pr = Prandtl number
 Re = Reynolds number
 Sc = Schmidt number
 T = temperature
 V = velocity vector
 W = molecular weight
 Y_n = concentration of species n
 y_n = mass fraction of species n
 ν = stoichiometric coefficient
 ρ = density
 Ψ = stream function
 Ω = vorticity
 ω_n = rate of production of species n

Subscripts

0 = inlet condition
 n = species

I. Introduction

THE numerical integration of the nonlinear differential equations governing the steady flow of a chemically reactive gas can present a severe numerical stability problem. This problem arises because of the relative stiffness of some of the chemical rate equations. For one-dimensional flows, if a conventional explicit numerical integration technique, e.g., Runge-Kutta or Adams-Moulton is used, stability considerations will force the use of an impractically small step size and result in excessive computation time.

Several attempts have been made to alleviate this problem.^{1,2} One approach to circumvent this difficulty is a method similar to that proposed by Treanor,³ wherein a conventional explicit numerical integration technique is modified to increase its stability and thus permits a larger step size to be employed.

Another way of overcoming the stability problem is to locally linearize the original equations at each step and then to apply an implicit method to the resulting linear equations. This would result in a stable scheme, but at the price of increased computational complexity.

The one-dimensional chemically reacting flowfield, neglecting viscosity, diffusion, and thermal conductivity have been solved by Pergament,⁴ using a Runge-Kutta with a variable time step increment, and by Emanuel,⁵ using a predictor-corrector method. Moretti⁶ pointed out that integration techniques for nonlinear, ordinary differential equations based on Runge-Kutta or similar methods are handicapped by the maximum step size Δt permissible for stability. Consequently, excessively large numbers of steps must be taken to perform the analysis of a process, forcing the computation of a two-dimensional flow with several streamlines impractical on economic grounds. Subsequently Moretti approximated the system of nonlinear equations describing a one-dimensional reacting flow by a linear non-homogeneous system. Unfortunately, in general, the eigenvalues for the solution may be complex, which increases the difficulty of obtaining the exact solution to the point where it renders the method impractical for a large system.

DeGroat and Abbett⁷ have proposed to approximate the solution to Moretti's system and these authors contend that the most important feature of this method is that it is not limited by a stability criteria, as is the case for the Runge-Kutta. Both this method and the method of Moretti are at least one to two orders of magnitude faster than the Runge-Kutta in the computational time, and in certain cases are even several orders of magnitude faster. Their intrinsic stability allows larger step sizes to be taken in applications of the one-dimensional chemical computations to two-dimensional fluid flow problem with finite-rate chemistry.

Lomax and Bailey² have pointed out that Moretti's method is neither more accurate nor more stable than their implicit method. The difficulties with Moretti's approach is that, even if the time steps are larger, the numerical determination of the eigenvalues of a matrix at each step enormously increases the complexity of the numerical computations. Bailey⁸ introduced the concept of parasitic eigenvalues in the numerical solution of the set of ordinary differential equations.

More recently, the solution of the time dependent reacting flow equations using explicit finite-difference approaches have been obtained. The steady-state problem is approached at large times. Most of the development of this approach has been directed towards examining the quasi-one-dimensional flow through a nozzle.⁹⁻¹¹ More recently this time dependent approach, using predictor corrector methods, has been applied to a two-dimensional reacting flow[‡] (see Ref. 12).

The following work examines two techniques for solving stiff type equations in steady multidimensional flows: relaxation and quasi-linearization of the species production rates. The latter method, based on Moretti's work,⁶ was found to be superior

Received November 16, 1973; presented as Paper 74-151 at the AIAA 12th Aerospace Sciences Meeting, Washington, D.C., January 30-February 1, 1974; revision received March 11, 1974.

Index categories: Combustion in Gases; Computer Technology and Computer Simulation Techniques.

* Staff Engineer, Linde Division.

† Associate Professor, Faculty of Engineering and Applied Sciences. Associate Fellow AIAA.

‡ We are indebted to a referee for pointing out this work.

to the relaxation approach. Results will be applied to the hydrogen-oxygen reaction in a two-dimensional flowfield.

II. Formulation

If one invokes the Shvab-Zeldovich approximations,^{1,3} the continuity and momentum equations may be uncoupled from the equations for conservation of species and energy. When this is done, the former equations may be solved first by a variety of approaches^{14,15} and their results used in the solution of the latter equations.

The nondimensional form of the governing equations, expressed in vector form in terms of the stream function Ψ and vorticity Ω , may be written in the following form¹⁴:

$$\begin{aligned}\nabla^2 \Psi &= -\Omega \\ \nabla^2 \Omega &= Re(V \cdot \nabla \Omega) \\ \nabla^2 T &= Re Pr \left[V \cdot \nabla T + \left(\frac{L}{\rho C_p V_0 T_0} \right) \sum_i h_i \omega_i \right] \\ \nabla^2 y_i &= Re Sc \left[V \cdot \nabla y_i + \left(\frac{L}{\rho V_0} \right) \omega_i \right]\end{aligned}$$

It can be shown that through the use of up-wind differences, the nonlinearity appearing in the convective terms can be forced to be stable.^{14,15} Using this one-sided difference approximation, the energy and species equations can be written, respectively, as

$$\begin{aligned}T_{i,j} &= \frac{1}{4} [T_{i+1,j} + T_{i,j+1} + T_{i-1,j} + T_{i,j-1}] - \\ &\quad \frac{Re}{8} \left[(\Psi_{i,j+1} - \Psi_{i,j-1}) \beta_1 - (\Psi_{i+1,j} - \Psi_{i-1,j}) \beta_2 \right] - \\ &\quad \frac{Re}{8} \left[\left(\sum_{i=1}^N h_i^0 \omega_{i,j}^n \right) \frac{L}{\rho C_p V_0 T_0} \right] \frac{\Delta x^2}{4} \quad (1)\end{aligned}$$

and

$$\begin{aligned}y_{i,j}^n &= \frac{1}{4} [y_{i+1,j}^n + y_{i,j+1}^n + y_{i-1,j}^n + y_{i,j-1}^n] - \\ &\quad \frac{Re}{8} \left[(\Psi_{i,j+1} - \Psi_{i,j-1}) \alpha_n - (\Psi_{i+1,j} - \Psi_{i-1,j}) \alpha_2 \right] + \\ &\quad \frac{\Delta x^2}{4} \left[\left(\frac{\omega_{i,j}^n}{\rho} \right) \left(\frac{L}{V_0} \right) \right] \quad (2)\end{aligned}$$

$n = 1, \dots, N$ (species)

where in Eqs. (1) and (2) when

$$\begin{aligned}[\Psi_{i+1,j} - \Psi_{i-1,j}] &\geq 0; \beta_2 = (T_{i,j+1} - T_{i,j}) \text{ or } \alpha_2 = (y_{i,j+1}^n - y_{i,j}^n) \\ [\Psi_{i+1,j} - \Psi_{i-1,j}] &< 0; \beta_2 = (T_{i,j} - T_{i,j-1}) \text{ or } \alpha_2 = (y_{i,j}^n - y_{i,j-1}^n) \\ [\Psi_{i,j+1} - \Psi_{i,j-1}] &\geq 0; \beta_1 = (T_{i,j} - T_{i-1,j}) \text{ or } \alpha_1 = (y_{i,j}^n - y_{i-1,j}^n) \\ [\Psi_{i,j+1} - \Psi_{i,j-1}] &< 0; \beta_1 = (T_{i+1,j} - T_{i,j}) \text{ or } \alpha_1 = (y_{i+1,j}^n - y_{i,j}^n)\end{aligned} \quad (3)$$

and where i, j = grid points.

However, the usual dominant source of instability in Eqs. (1) and (2) is the rate of change of the mass fraction $\omega_{i,j}^n = y_{i,j}^n$, described as

$$\begin{aligned}\dot{y}_{i,j}^n &= W^n \sum_{k=1}^M (v_{n,k}' - v_{n,k}'') k_f \left\{ \prod_{n=1}^N [(y_{i,j}^n \cdot \rho) / W^n]^{v_{n,k}'} - \right. \\ &\quad \left. \frac{1}{K_c} \prod_{n=1}^N [(y_{i,j}^n \cdot \rho) / W^n]^{v_{n,k}''} \right\} \quad (4a) \\ k &= 1, \dots, M \text{ (reactions)} \\ n &= 1, \dots, N \text{ (species)}\end{aligned}$$

where v_n' and v_n'' are the usual stoichiometric coefficients, k_f and k_b are the forward and backward reactions rates. The rate of change of the concentration of species n and reaction k could also be expressed as

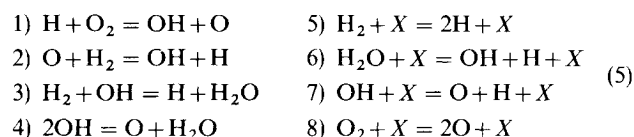
$$\dot{Y}_{n,k} = k_f^k \prod_{n=1}^N Y_n^{v_n'} - k_b^k \prod_{n=1}^N Y_n^{v_n''} \quad (4b)$$

where the total rate of change of the concentration of species 1 caused by all chemical reaction is

$$\dot{Y}_n = \sum_{k=1}^M \dot{Y}_{n,k} \quad (4c)$$

Equation (4b) forms a system of nonlinear, stiff, ordinary differential equations. If we apply our implicit method, described by Eqs. (1) and (2), with the rate of change of mass fraction $\omega_{i,j}^n$ given by Eq. (4), instabilities in the numerical solution normally will result. In fact, when complex systems are involved, "explosive" divergence appears. This type of instability is characterized by a rapid and unbounded divergence of the solution within two or three iterations.

As an example for solving these stiff equations, the H_2 - O_2 reaction in a two-dimensional flowfield was examined. For this reaction, six different species will be involved: H , O , H_2O , OH , O_2 , and H_2 (these species will be referred, respectively, as 1, 2, 3, 4, 5, 6). Based upon Pergament's work,⁴ eight reactions mechanisms will be assumed



where X is a catalyst. Equation (4b) then reads for these species, $\dot{Y}_{i,k}$, where i is the chemical species and k is the reaction number

$$\begin{aligned}\dot{Y}_{21} &= k_{f1} Y_1 Y_5 - k_{b1} Y_2 Y_4 & \dot{Y}_{34} &= \dot{Y}_{24} \\ \dot{Y}_{12} &= k_{f2} Y_2 Y_6 - k_{b2} Y_1 Y_4 & \dot{Y}_{65} &= -\frac{1}{2} \dot{Y}_{15} \\ \dot{Y}_{13} &= k_{f3} Y_6 Y_4 - k_{b3} Y_1 Y_3 & \dot{Y}_{46} &= \dot{Y}_{16} \\ \dot{Y}_{24} &= k_{f4} Y_4^2 - k_{b4} Y_2 Y_3 & \dot{Y}_{27} &= \dot{Y}_{17} \\ \dot{Y}_{15} &= k_{f5} Y_6 Y_x - k_{b5} Y_1^2 Y_x & \dot{Y}_{58} &= -\frac{1}{2} \dot{Y}_{28} \\ \dot{Y}_{16} &= k_{f6} Y_3 Y_x - k_{b6} Y_1 Y_4 Y_x & \dot{Y}_{11} &= \dot{Y}_{51} = -\dot{Y}_{21} \\ \dot{Y}_{17} &= k_{f7} Y_4 Y_x - k_{b7} Y_1 Y_2 Y_x & \dot{Y}_{22} &= \dot{Y}_{62} = -\dot{Y}_{12} \\ \dot{Y}_{28} &= k_{f8} Y_5 Y_x - k_{b8} Y_2^2 Y_x & \dot{Y}_{63} &= \dot{Y}_{43} = -\dot{Y}_{13} \\ \dot{Y}_{41} &= \dot{Y}_{21} & \dot{Y}_{44} &= -2 \dot{Y}_{24} \\ \dot{Y}_{42} &= \dot{Y}_{12} & \dot{Y}_{36} &= -\dot{Y}_{16} \\ \dot{Y}_{33} &= \dot{Y}_{13} & \dot{Y}_{47} &= -\dot{Y}_{17}\end{aligned} \quad (6)$$

where Y_x is the concentration of the catalyst. After invoking an atom conservation for oxygen and hydrogen, the total rate of change of the concentrations of species 1 for the reaction Eq. (5) reduces to four equations

$$\begin{aligned}\dot{Y}_1 &= \dot{Y}_{11} + \dot{Y}_{12} + \dot{Y}_{13} + \dot{Y}_{15} + \dot{Y}_{16} + \dot{Y}_{17} \\ \dot{Y}_2 &= \dot{Y}_{21} - \dot{Y}_{12} + \dot{Y}_{24} + \dot{Y}_{17} + \dot{Y}_{28} \\ \dot{Y}_3 &= \dot{Y}_{13} + \dot{Y}_{24} - \dot{Y}_{16} \\ \dot{Y}_4 &= \dot{Y}_{21} + \dot{Y}_{12} - \dot{Y}_{13} - 2 \dot{Y}_{24} + \dot{Y}_{16} - \dot{Y}_{17}\end{aligned} \quad (7)$$

with the rate of change of concentration for O_2 and H_2 expressed by Eq. (6)

$$\dot{Y}_5 = -\frac{1}{2} [\dot{Y}_2 + \dot{Y}_4 + \dot{Y}_3]; \quad \dot{Y}_6 = -\frac{1}{2} [\dot{Y}_1 + \dot{Y}_4 + 2 \dot{Y}_3] \quad (8)$$

Two approaches will be examined in solving these stiff equations (4b) or (6); an under-relaxation technique and a quasi-linearization technique.

III. Under-Relaxation.

The dependent variables $T_{i,j}$ and $Y_{i,j}$ may be underrelaxed after each iteration by simply writing

$$\phi_{i,j}^{NEW} = \phi_{i,j}^{OLD} + r(\phi_{i,j}^{NEW} - \phi_{i,j}^{OLD}) \quad (9)$$

where r is the relaxation parameter. However, this procedure would increase manifold the number of iterations necessary before convergence is obtained and it would be more appropriate to underrelax directly the source of divergence after each iteration. Therefore the following modification was performed.

In Eq. (3), one observed that any error introduced in the solution will be amplified by the terms $(y)''$ and $(y)'''$. These terms prove to be very "sensitive," particularly when the reaction involves a trimolecular collision. Improvement of the relaxation approach was found to occur when the rate of change of mass fraction was underrelaxed by replacing the terms in Eq. (4) with

$$(y)''^{[r - (\Delta r)n]} \quad \text{and} \quad (y)'''^{[r - (\Delta r)n]} \quad (10)$$

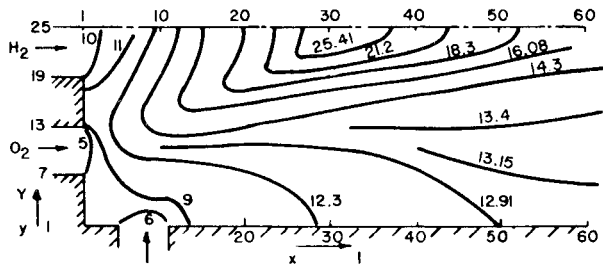


Fig. 1 Constant temperature contour, 10^3 °K, nonequilibrium flow, adiabatic boundary conditions.

Here r is the relaxation parameter, Δr is an arbitrary incremental change in r , and n is the iteration counter. In effect, all the stoichiometric coefficients in the reaction rates are multiplied by a common factor r . After $(r-1)/\Delta r$ iterations the relaxation parameter returns to one, and all stoichiometric coefficients return to their initial value. For the H_2O_2 reaction, r was selected to be 1.5 and Δr was set to 0.005. The choice of relaxation factor is a trial and error procedure, since it really depends on the "stiffness" of the equations. The solution was assumed to have converged when the set of difference equations was satisfied to an order of 10^{-5} and when

$$\sum_{i=1}^N Y_{i,j}^n = 1$$

at various selected grid locations. Both requirements were satisfied during the iteration procedure at the same rate of convergence, so that either one was sufficient. The computational time per iteration was reduced considerably (by a factor of four) when the rate of change of mass fraction was calculated only at preselected grid locations, and the values at the neighboring locations is interpolated. The rate of change was calculated for 90 equally spaced grid points, and the values at the intermediate locations were linearly interpolated from the known values. Using this coarse grid approach the solution converged in 450 iterations and 1230 sec on the CDC 6400.

IV. Quasi-Linearization

The set of "stiff" equations (7) can be quasi-linearized and reduced to a linear system of equations by expressing the product $(Y_m Y_n)$ in Eq. (6) as

$$Y_m Y_n = -Y_m^0 Y_n^0 + Y_m^0 Y_n + Y_n^0 Y_m \quad (11)$$

where $(^0)$ refers to the previous iteration. After substituting into Eqs. (7) and (8) one obtains the approximated system of linear, nonhomogeneous equations

$$\dot{Y}_m = \sum a_{mn} Y_n + C_m \quad (m, n = 1, 2, 3, 4) \text{ species} \quad (12)$$

where a_{mn} are given by⁶

$$\begin{aligned} a_{11} &= k_{f1}[-b + (Y_2 + Y_4 + Y_3)/2] - (k_{f2} Y_2 + k_{f3} Y_4)/2 - \\ &\quad [k_{b2} Y_4 + k_{b3} Y_3 + Y_x k_{f5}/2 + k_{b6} Y_4 + k_{b7} Y_2 Y_x] - 2k_{b5} Y_1 Y_x \\ a_{12} &= k_{f2}[c - (Y_1 + Y_4 + 2Y_3)/2] + Y_1(k_{f1}/2 - k_{b7} Y_x) + k_{b1} Y_4 \\ a_{13} &= k_{f1} Y_1/2 - (k_{f2} Y_2 + k_{f3} Y_4 + k_{b3} Y_1) + (k_{f6} - k_{f5}) Y_x \end{aligned}$$

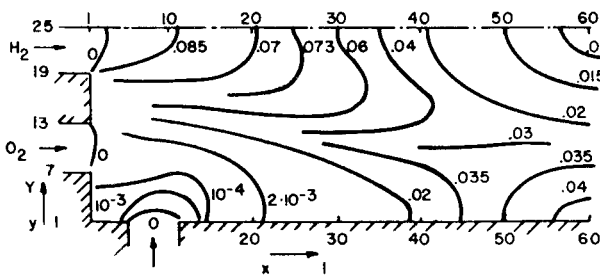


Fig. 2 H_2 constant weight fraction contour, nonequilibrium flow.

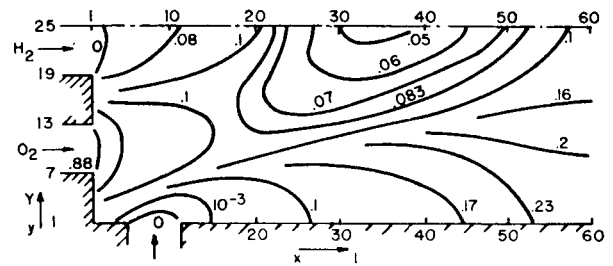


Fig. 3 O_2 constant weight fraction contour, nonequilibrium flow.

$$\begin{aligned} a_{14} &= k_{f3}[c - Y_1/2 - (Y_3 + Y_4)] + (k_{f1} Y_1 - k_{f2} Y_2)/2 + \\ &\quad [k_{b2} Y_2 - k_{b2} Y_1 + Y_x(k_{f7} - k_{f5}/2 - k_{b6} Y_1)] \\ a_{21} &= k_{f1}[b - (Y_2 + Y_3 + Y_4)/2] + (k_{f2}/2 - k_{b7} Y_x) Y_2 + k_{b2} Y_4 \\ a_{22} &= k_{f2}[c - (Y_1 + Y_4 + 2Y_3)/2] - (k_{f1}/2 + k_{b7} Y_x) Y_1 - \\ &\quad (k_{b1} Y_4 + k_{b4} Y_3) - (k_{f8}/2 + 2k_{b8} Y_2) Y_x \\ a_{23} &= -k_{f1} Y_1/2 + (k_{f2} - k_{b4}) Y_2 - k_{f8} Y_x/2 \\ a_{24} &= (k_{f2} Y_2 - k_{f1} Y_1)/2 + (k_{b2} Y_1 - k_{b1} Y_2) + 2k_{f4} Y_4 + \\ &\quad (k_{f7} - k_{f8}/2) Y_x \\ a_{31} &= (k_{b6} Y_x - k_{f3}/2) Y_4 - k_{b3} Y_3 \\ a_{32} &= -k_{b4} Y_3 \\ a_{33} &= -(k_{f8} Y_4 + k_{b3} Y_1 + k_{b4} Y_2 + k_{f6} Y_x) \\ a_{34} &= k_{f3}[c - (Y_1 + 2Y_4 + 2Y_3)/2] + 2k_{f4} Y_4 + k_{b6} Y_1 Y_x \\ a_{41} &= k_{f1}[b - (Y_2 + Y_3 + Y_4)/2] + (-k_{f2}/2 + k_{b7} Y_x) Y_2 + \\ &\quad (k_{f3}/2 - k_{b2} - k_{b6} Y_x) Y_4 + k_{b3} Y_3 \\ a_{42} &= k_{f2}[c - (Y_1 + Y_4 + 2Y_3)/2] + (k_{b7} Y_x - k_{f1}/2) Y_1 - \\ &\quad k_{b1} Y_4 + 2k_{b4} Y_3 \\ a_{43} &= (k_{b3} - k_{f1}/2) Y_1 + (2k_{b4} - k_{f2}) Y_2 + k_{f3} Y_4 + k_{f6} Y_x \\ a_{44} &= -k_{f3}[c - Y_1/2 - (Y_3 + Y_4)] - [k_{f1}/2 + k_{b2} + k_{b6} Y_x] Y_1 - \\ &\quad (k_{b1} + k_{f2}/2) Y_2 - 4k_{f4} Y_4 - k_{f7} Y_x \\ c_1 &= (k_{f2} Y_2 + k_{f3} Y_4)[(Y_1 + Y_4)/2 + Y_3] + k_{b2} Y_1 Y_4 - \\ &\quad k_{f1} Y_1(Y_2 + Y_3 + Y_4)/2 - k_{b1} Y_2 Y_4 + k_{b3} Y_1 Y_3 + \\ &\quad (k_{b6} Y_4 + k_{b5} Y_1 + k_{b7} Y_2) Y_1 Y_x + k_{f5} Y_x c \\ c_2 &= k_{f1} Y_1(Y_2 + Y_3 + Y_4)/2 + k_{b1} Y_2 Y_4 - \\ &\quad k_{f2} Y_2[(Y_1 + Y_4)/2 + Y_3] - k_{b2} Y_1 Y_4 - k_{f4} Y_4^2 + k_{b4} Y_2 Y_3 + \\ &\quad (k_{b7} Y_1 + k_{b8} Y_2) Y_2 Y_x + k_{f8} Y_x b \\ c_3 &= k_{f3} Y_4[(Y_1 + Y_4)/2 + Y_3] + k_{b3} Y_1 Y_3 - k_{f4} Y_4^2 + \\ &\quad k_{b4} Y_2 Y_3 - k_{b6} Y_4 Y_1 Y_x \\ c_4 &= k_{f1} Y_1(Y_2 + Y_3 + Y_4)/2 + k_{b1} Y_2 Y_4 + \\ &\quad (k_{f2} Y_2 - k_{f3} Y_4)[(Y_1 + Y_4)/2 + Y_3] + k_{b2} Y_1 Y_4 - \\ &\quad k_{b3} Y_1 Y_3 + 2k_{f4} Y_4^2 - 2k_{b4} Y_2 Y_3 + (k_{b6} Y_4 - k_{b7} Y_2) Y_1 Y_x \\ b &= \left(Y_5 + \frac{Y_2 + Y_3 + Y_4}{2} \right)^0 \quad c = \left(Y_6 + Y_3 + \frac{Y_1 + Y_4}{2} \right)^0 \end{aligned}$$

Also

$$\begin{aligned} Y_5 &= -\frac{Y_2 + Y_3 + Y_4}{2} + \left(Y_5 + \frac{Y_2 + Y_3 + Y_4}{2} \right)^0 \\ Y_6 &= -\frac{Y_1 + Y_4}{2} - Y_3 + \left(Y_6 + Y_3 + \frac{Y_1 + Y_4}{2} \right)^0 \end{aligned}$$

and the forward and backward reaction rate coefficients are given in Table 1.

Performing this quasi-linearization procedure, Eqs. (7) and (8) are evaluated and introduced into Eqs. (1) and (2). The resulting

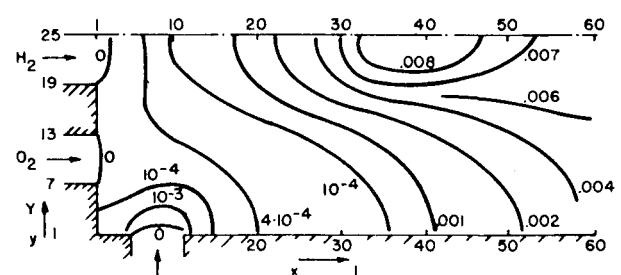


Fig. 4 H constant weight fraction contour, nonequilibrium flow.

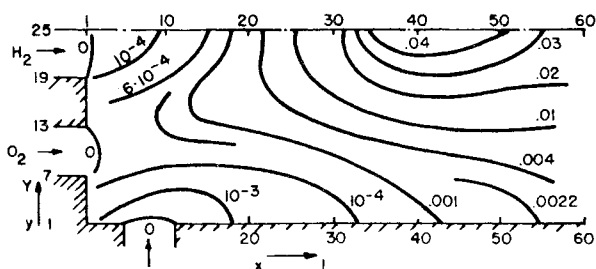


Fig. 5 O constant weight fraction contour, nonequilibrium flow.

Table 1 Reaction rate for H₂-O₂ System⁶

$k_{f1} = 3 \times 10^{14} e^{-8.81/T}$	$k_{b1} = 2.48 \times 10^{13} e^{-0.66/T}$
$k_{f2} = 3 \times 10^{14} e^{-4.03/T}$	$k_{b2} = 1.30 \times 10^{14} e^{-2.49/T}$
$k_{f3} = 3 \times 10^{14} e^{-3.02/T}$	$k_{b3} = 1.33 \times 10^{15} e^{-10.95/T}$
$k_{f4} = 3 \times 10^{14} e^{-3.02/T}$	$k_{b4} = 3.12 \times 10^{15} e^{-12.51/T}$
$k_{f5} = 1.85 \times 10^{17} e^{-54/T}$	$k_{b5} = 10^{16}$
$k_{f6} = 9.66 \times 10^{18} e^{-62.2/T}$	$k_{b6} = 10^{17}$
$k_{f7} = 8 \times 10^{16} e^{-52.2/T}$	$k_{b7} = 10^{16}$
$k_{f8} = 5.8 \times 10^{16} e^{-60.6/T}$	$k_{b8} = 6 \times 10^{14}$

^a *T* is the absolute temperature in K, divided by 1000. The rate coefficients k_{fi} and k_{bi} are in mole/(cm³-sec), except for k_{b5} , k_{b6} , k_{b7} , and k_{b8} which are in mole²/(cm³-sec). These data have been assumed according to Ferri et al.¹⁷

set of simultaneous algebraic equations were solved by a Gauss-Seidel type of procedure without any additional difficulties arising. The numerical scheme was not affected by the "explosive" divergence previously encountered.

It should be noted that it is possible to include a temperature effect term in the expansion of the production term in the iteration dimension. At the suggestion of a referee, we briefly examined the inclusion of a temperature dependence and it appears that convergence can be improved. This would be especially helpful for cases where poor estimates were made of the initial temperatures.

Using the above approach on a 60 × 25 mesh point grid, convergence was obtained in 320 iterations and 737 sec on the CDC 6400.

V. Discussion

Both methods have been used by the authors in multi-dimensional flow problems utilizing a variety of chemical reactions. When applied to the two-dimensional flowfield with H₂O₂ combustion, both the under-relaxation and the quasi-linearization ultimately yield the same distributions and similar mass fraction results. Representative results are given for the case of adiabatic wall conditions, and discrete injection of an inert dilutant. The mass fractions of the hydrogen, oxygen, and inert dilutant are, respectively, 0.12, 0.88, and 0.06. The inlet vorticity of the oxygen was taken to be +15.

The transport parameters employed in this work were calculated using a variation of the method described in Ref. 18.

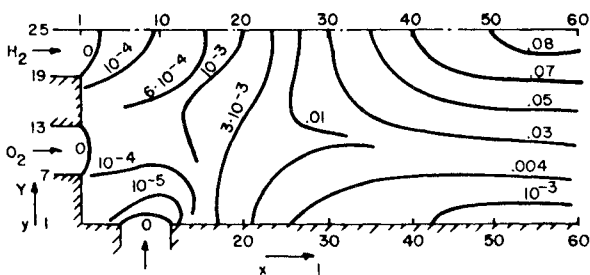


Fig. 6 OH constant weight fraction contour, nonequilibrium flow.

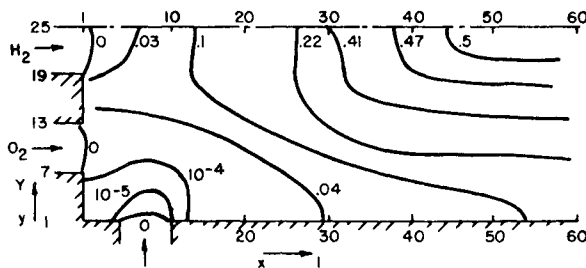


Fig. 7 H₂O constant weight fraction contour, nonequilibrium flow.

After calculating the thermodynamic data for each species, a least-square technique was used to fit the data into polynomials and used to determine the appropriate transport parameters.

Figure 1 gives the temperature profiles. Maximum temperature profiles occur at about 30 grid units downstream and are symmetric about the centerline axis. This corresponds to the stoichiometric mixture of H₂ + O₂.

The hydrogen concentration decreases continuously along the central axis of the combustor, Fig. 2. At the exit plane the mass fraction value of the hydrogen is four times higher at the wall than at the centerline and can be attributed to incomplete burning due to the cooling effect of the dilutant gas.

As a result of the inlet vorticity, the oxygen mixes with the hydrogen quite rapidly (Fig. 3). A plot of the oxygen concentration along the centerline shows an increase in the O₂ mass

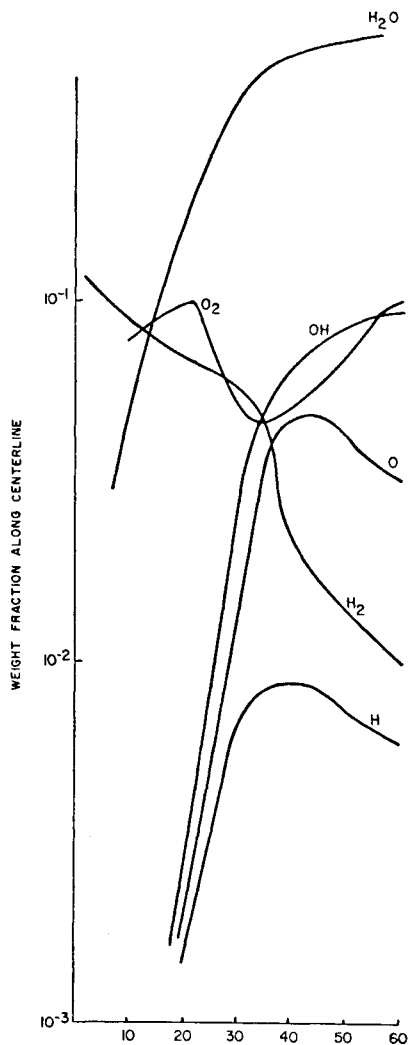


Fig. 8 Centerline dimensional distance (grid spacing).

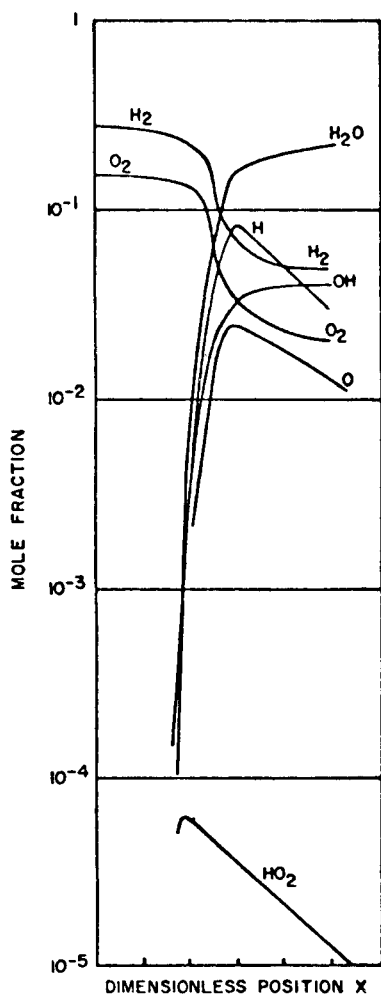


Fig. 9 1-D results from Bittker and Schulin mole fractions vs position.

fraction from 0 to 0.1 over the first 20 units with subsequent decay to a minimum value of approximately 0.5 near the maximum temperature region. In this region the hydrogen reacts with O_2 and the temperature continuously increases. Downstream of the 40 dimensionless units region, oxygen is being radially brought into the centerline due to the two-dimensional mixing and the O_2 concentration increases. At the same time the temperature begins to decay because of dilution effects. The concentration of free hydrogen and atomic oxygen is seen to peak slightly downstream from the maximum temperature region (Figs. 4–5). Since the production of such species is favored by temperature increases, these results are consistent with equilibrium predictions and compatible with van Hoff's equation. The concentration of hydroxyl radical continuously increases as the reaction and the flow proceeds downstream, OH being principally formed in the post flame region (Fig. 6). The same is true for the concentration of water vapor. Both concentrations decay near the wall due to lower reaction rates occurring in this region. The centerline concentrations are summarized in Fig. 7. Qualitatively these results are compatible with earlier work,¹⁶ with the exception of the centerline behavior of O_2 which is due to the inclusion of the two-dimensional mixing effects (Fig. 8). The one-dimensional results of Bittker and Scullin¹⁶ are shown in Fig. 9 for qualitative comparisons. Both show atomic hydrogen and oxygen peaking in the flame region and rapidly decaying thereafter. The hydroxyl radical, OH, and water vapor concentrations trends of forming in the post flame region and then remaining approximately constant are also shown in both studies.

As mentioned at the beginning of this discussion, both under-relaxation and quasi-linearization yield essentially the same

results. However, in the former, the choice of the relaxation factor (r) is a trial and error procedure which normally is time consuming and for many reactions demands judicious adjustments of (r). The quasi-linearization approach eliminates all these requirements and obtains results in a straightforward manner. Most importantly, when quasi-linearization was employed, computational time was reduced by several orders of magnitude from that required by underrelaxation. The quasi-linearization procedure appears to be very useful for multi-dimensional flows, where many species and reaction steps are involved. Presently this scheme is being successfully employed in modeling hydrocarbon oxidation in multidimensional combustors.¹⁴

References

- ¹ Curtiss, C. F. and Hirschfelder, J. O., "Integration of Stiff Equations," *Proceedings of the National Academy of Science*, Vol. 28, 1952, pp. 235–243.
- ² Lomax, H. and Bailey, H. E., "A Critical Analysis of Various Numerical Integration Methods for Computing the Flow of a Gas in Chemical Non-Equilibrium," TN D-4109, 1967, NASA.
- ³ Treanor, C. E., "A Method for the Numerical Integration of Coupled First Order Differential Equations with Greatly Different Time Constants," *Mathematics of Computation*, Vol. 29, No. 93, Jan. 1966, pp. 39–45.
- ⁴ Pergament, H. S., "A Theoretical Analysis of Nonequilibrium Hydrogen-Air Reactions in Flow Systems," AIAA Paper 63-113, White Oak, Md., 1963.
- ⁵ Emanuel, G., "Problems Underlying the Numerical Integration of Chemically and Vibrational Rate Equations in a Non-Equilibrium Flow," AEDC Rept. TDR-63-82, March 1963, Arnold Engineering Development Center, Tullahoma, Tenn.
- ⁶ Moretti, G., "A New Technique for Numerical Analysis of Non-equilibrium Flows," *AIAA Journal*, Vol. 3, No. 2, Feb. 1965, pp. 223–229.
- ⁷ DeGroat, J. J. and Abbett, M. J., "A Computation of One-Dimensional Combustion of Methane," *AIAA Journal*, Vol. 3, No. 2, Feb. 1965, pp. 381–383.
- ⁸ Bailey, H. E., "Numerical Integration of the Equations Governing the One-Dimensional Flow of a Chemically Reactive Gas," *The Physics of Fluids*, Vol. 12, No. 11, Nov. 1969, pp. 2292–2300.
- ⁹ Anderson, J. D., Jr., "A Time-Dependent Analysis for Vibrational and Chemical Nonequilibrium Nozzle Flows," *AIAA Journal*, Vol. 8, No. 3, March 1970, pp. 545–550.
- ¹⁰ Vamos, J. S. and Anderson, J. D., Jr., "Time Dependent Solutions of Nonequilibrium Nozzle Flows—A Sequel," *AIAA Journal*, Vol. 8, No. 12, Dec. 1970, pp. 2280–2282.
- ¹¹ Vamos, J. S. and Anderson, J. D., Jr., "Time Dependent Analysis of Nonequilibrium Nozzle Flows with Complex Chemistry," *Journal of Spacecraft and Rockets*, Vol. 10, No. 4, April 1973, pp. 225–226.
- ¹² Li, C. P., "Hypersonic Nonequilibrium Flow past a Sphere at Low Reynolds Numbers," AIAA Paper 74-173, Washington, D.C., 1974.
- ¹³ Williams, F. A., *Combustion Theory*, Addison-Wesley, Reading, Mass., 1965.
- ¹⁴ Kennedy, L. A. and Scaccia, C., "Modeling of Gas Turbine Combustors," presented at the International Conference on Numerical Methods in Fluid Dynamics, Sept. 1973, Southampton Univ., Southampton, England.
- ¹⁵ Scaccia, C. and Kennedy, L. A., "Mixing of Coaxial Jets in a Confined Tube," *Developments in Mechanics, Proceedings of the 13th Midwestern Mechanics Conference*, Vol. 7, University of Pittsburgh, Pittsburgh, Pa., Aug. 1973, pp. 95–110.
- ¹⁶ Bittker, D. A. and Scullin, V. J., "General Chemical Kinetic Computer Program for Static and Flow Reactions, with Applications to Combustion and Shock-Tube Kinetics," TN D-6586, Jan. 1972, NASA.
- ¹⁷ Ferri, A., Libby, P. A., and Zakkay, V., "Theoretical and Experimental Investigation of Supersonic Combustion," presented at the Third ICAS Congress, Stockholm, Sweden, Aug. 1962.
- ¹⁸ Svehla, R. A. and McBride, B. J., "Fortran IV Computer Program for Calculation of Thermodynamic and Transport Properties of Complex Chemical Systems," TN D-7056, Jan. 1973, NASA.